Published in final edited form as:

Cereb Cortex. 2025 August 01; 35(8): . doi:10.1093/cercor/bhaf220.

Longitudinal magnetic resonance imaging reveals differences in cortical expansion in fetuses with congenital heart defects

Kara E. Garcia[1,2,*], **Kaylin Taylor**[3], **Meghana Bhaskara**[4], **Clemente Velasco-Annis**[5], **John Vieth**[6], **Joshua Garrett**[7], **Jessica Patel**[7], **Benjamin Pointer**[7], **Sha Cao**[8], **Jane W. Newburger**[9,10], **Ali Gholipour**[11,12], **Caitlin K. Rollins**[13,14], **Cynthia M. Ortinau**[7]

[1]Department of Radiology & Imaging Sciences, Indiana University School of Medicine, Evansville, IN, USA

[2]Department of Mechanical Engineering & Materials Science, Washington University, St. Louis, MO, USA

[3]Department of Neurology, Washington University, St. Louis, MO, USA

[4]Indiana University School of Medicine, Evansville, IN, USA

[5]Department of Radiology, Boston Children's Hospital, Boston, MA, USA

[6]University of Kentucky College of Medicine, Lexington, Lexington, KY, USA

[7]Department of Pediatrics, Washington University, St. Louis, MO, USA

[8]Department of Biostatistics and Health Data Science, Center for Computational Biology and Bioinformatics, Indiana University School of Medicine, Indianapolis, IN, USA

[9]Department of Cardiology, Boston Children's Hospital, Boston, MA, USA

[10]Department of Pediatrics, Harvard Medical School, Boston, MA, USA

[11]Department of Radiological Sciences, School of Medicine, University of California Irvine, Irvine, CA, USA

[12]Department of Electrical Engineering and Computer Science, School of Engineering, University of California Irvine, Irvine, CA, USA

[13]Department of Neurology, Harvard Medical School, Harvard Medical School, Boston, MA, USA

[*]Corresponding Author: Indiana University School of Medicine, 515 Bob Jones Way, Evansville, IN 47708, karagarc@iu.edu.

Author Contributions

Kara Garcia (Conceptualization, Formal analysis, Investigation, Methodology, Software, Supervision, Visualization, Writing - original draft, Writing - review & editing), Kaylin Taylor (Data curation, Formal analysis, Methodology, Project administration, Visualization, Writing - original draft, Writing - review & editing), Meghana Bhaskara (Formal analysis, Visualization, Writing - original draft, Writing - review & editing), Clemente Velasco-Annis (Formal analysis, Resources, Software, Writing - review & editing), John Vieth (Formal analysis, Writing - review & editing), Joshua Garrett (Formal analysis, Writing - review & editing), Jessica Patel (Formal analysis, Writing - review & editing), Benjamin Pointer (Formal analysis, Writing - review & editing), Sha Cao (Formal analysis, Writing - review & editing), Jane Newburger (Writing - review & editing), Ali Gholipour (Formal analysis, Methodology, Software, Writing - review & editing), Caitlin Rollins (Conceptualization, Data curation, Methodology, Resources, Writing - review & editing), and Cynthia Ortinau (Conceptualization, Data curation, Formal analysis, Funding acquisition, Investigation, Methodology, Project administration, Resources, Supervision, Writing - original draft, Writing - review & editing).

Conflicts of Interest

The authors have no conflicts of interest.

Author Manuscript

Author Manuscript

Author Manuscript

[14]Department of Neurology, Boston Children's Hospital, Harvard Medical School, Boston, MA, USA

Abstract

For children with congenital heart disease (CHD), differences in brain structure are already present at birth. Cortical surface area and gyrification increase dramatically over the third trimester, and cortical expansion has been hypothesized to drive brain folding. This study sought to quantify differences in cortical expansion in fetuses with CHD and typically developing controls. Fetal magnetic resonance imaging was conducted at early (26–31 weeks) and late (34–39 weeks) gestational time points, and cortical surfaces were reconstructed using a high resolution, motion-corrected pipeline. For fetuses with reconstructions at both time points (36 CHD, 24 control), anatomically-constrained multimodal surface matching (aMSM) was used to generate individualized maps of cortical surface expansion. Global analysis revealed significant reductions in total cortical expansion and gyrification index among CHD fetuses. Furthermore, expansion maps revealed high expansion in the lateral temporal lobes of control fetuses that was reduced in fetuses with CHD, consistent with previous reports of atypical folding in this region. This study is the first to reveal spatiotemporal patterns of cortical expansion in typical and atypical fetal development. This detailed understanding of cortical growth trajectory may improve understanding of functional deficits associated with specific cortical areas and inform clinical interventions for patients with CHD.

Keywords

Congenital heart disease; Cortical Expansion; Fetal development; Gyrification; Magnetic resonance imaging

---

The third trimester of pregnancy represents a crucial period of human brain development, during which total brain volume doubles (Andescavage et al. 2017) and outer surface area triples (Lefevre et al. 2016). In fetuses with complex congenital heart defects (CHD), the typical developmental trajectory of the fetal brain is altered, resulting in decreased total and regional brain volumes, abnormal sulcation, and altered brain metabolism (Clouchoux et al. 2013; Ortinau et al. 2019; Rollins et al. 2021; Andescavage et al. 2023). Divergence in brain structure persists postnatally, throughout childhood and adulthood, for patients with CHD (Ortinau et al. 2022). Moreover, a growing body of evidence has linked alterations in brain development with the neurodevelopmental and psychosocial impairments that occur in patients with CHD (Asschenfeldt et al. 2020; Ortinau et al. 2022; Sadhwani et al. 2022).

Advances in fetal magnetic resonance imaging (MRI) methods have improved our understanding of structural brain alterations that occur in fetuses with CHD. Limperopoulos and colleagues (Limperopoulos et al. 2010) were the first to report smaller intracranial and total brain volumes, as well as altered brain metabolism, in fetuses with CHD compared to controls. Subsequent regional brain analyses showed that both white and gray matter structures are affected, with transient fetal brain compartments appearing particularly vulnerable (Rollins et al. 2021). In addition to changes in brain size, differences in cortical morphology have been observed. Fetuses with CHD differ in terms of sulcal number, location, and pattern similarity (Ortinau et al. 2019). Alterations have also been reported in cortical depth and the timing in which sulci emerge (Clouchoux et al. 2013).

Cortical growth has been suggested as a driving factor in brain folding (Richman et al. 1975; Reillo et al. 2011; Kelly et al. 2012) and computational analyses suggest that cortical fold morphology may depend on the rate (Bayly et al. 2013) and spatial distribution (Richman et al. 1975) of growth. In preterm infants, patterns of cortical surface expansion during the third trimester equivalent correlate with regions undergoing active brain folding (Garcia et al. 2018). Thus, early divergence from the normal trajectory of cortical expansion could contribute to cortical folding abnormalities noted in brains of fetuses and infants with CHD. However, investigations into the spatial distributions of cortical growth during healthy fetal development have been limited, and none have explored patterns of fetal development for cases with known CHD.

In this study, we aim to quantify regional differences in cortical growth over the third trimester in fetuses with CHD compared to their control counterparts. We use recent advances in fetal MRI to precisely quantify cortical size and gyrification during the third trimester of pregnancy (Kainz et al. 2015; Gholipour et al. 2017; Dou et al. 2020). Moreover, by considering fetuses scanned at two time points within the third trimester (early and late), we are able to longitudinally track changes at the individual subject level. Using recently developed techniques to map growth across the cortical surface (Garcia et al. 2018), we reveal a distinct region of reduced cortical growth in fetuses with CHD. Results may offer insight into the neurobiological mechanism by which CHD is associated with regional brain maldevelopment and may guide future mechanistic studies.

Materials and Methods

Study Design and Participants

Pregnant women with and without a known diagnosis of fetal complex CHD were recruited from March 2014 to January 2022 into two ongoing prospective longitudinal fetal brain MRI studies, one conducted at St. Louis Children’s Hospital (SLCH) and the other at Boston Children’s Hospital (BCH). Across both sites, inclusion criteria were maternal age 18–45 years, singleton pregnancy, and either fetal complex CHD (cases) or a fetus with normal cardiac anatomy on fetal echocardiogram (controls), many of whom had family history of CHD. Exclusion criteria were fetal congenital infection, non-English speaking (SLCH only), significant maternal CHD, structural fetal brain malformation, contraindication to MRI, and termination or other scenarios in which approach was considered clinically inappropriate. For the current study, fetuses with known genetic syndromes or congenital anomalies were excluded. This determination was made based on fetal and postnatal clinical genetic testing, prenatal and postnatal imaging studies (e.g., screening abdominal ultrasound for midline evaluation), and physical examination after birth. Moreover, the current study only considered cases in which the full longitudinal set of fetal MRIs (2 scans) could be collected, and those who underwent their first fetal MRI prior to 26 weeks’ gestation (prior to emergence of sulcal landmarks necessary for cortical surface mapping) were excluded. Each study was approved by the local Institutional Review Board (Boston

Children's Hospital IRB IRB-P00008836 and Washington University in St. Louis IRB, IRB #201710214), and written informed consent was obtained from all participants.

Maternal and fetal demographic and clinical variables were collected through medical record review and participant questionnaires. To evaluate differences by cardiac anatomy, fetuses with CHD were grouped as hypoplastic left heart syndrome (HLHS), transposition of the great arteries (TGA), tetralogy of Fallot (TOF), or "Other CHD" based on fetal echocardiography.

Fetal MRI Acquisition and Post-processing

Participants underwent two fetal brain MRIs performed on a 3-Tesla Siemens scanner with similar acquisition parameters across both sites. T2-weighted half Fourier acquisition single shot turbo spin echo (T2wHASTE) sequences (Figure 1A) were obtained in the coronal, sagittal, and axial planes with a repetition time of 1400–2000 ms, echo time of 100–120 ms, 256 × 204, 256 × 256, or 320 × 320 acquisition matrices; 2–3 mm slice thickness and in-plane resolution of 1 mm. The T2wHASTE sequences from each fetus were reconstructed (Figure 1B) and automatically segmented (Figure 1C) using in-house software and fetal MRI pipelines as previously described (Rollins et al. 2021). Briefly, this involved the application of a motion corrected super-resolution volume reconstruction (Kainz et al. 2015) followed by signal normalization and nonuniformity correction, registration to a fetal brain MRI atlas, and application of an automated multi-atlas-based segmentation (Gholipour et al. 2017).

To generate cortical surfaces, the volumetric segmentation was simplified in ITK-Snap to approximate the boundary between the white matter and fetal cortex (www.ITKSnap.org; (Yushkevich et al. 2006); Figure 1D). The reconstructed anatomical images and simplified segmentation were then aligned along the anterior and posterior commissure and cropped into left and right hemispheres (Ortinau et al. 2013). The cropped segmentations were dilated from 0.0–0.2 iterations on a case-by-case basis to more closely approximate the cortical midthickness surface. Manual refinements were then made in ITK-Snap such that the border of the segmentation was at the level of the mid-cortex. All refined segmentations were reviewed by a single rater to ensure consistency and minimize inter-rater variability. Subjects were excluded from final analysis if MRI quality was deemed insufficient for segmentation at either time point. Based on the subjects with full datasets after quality control, it was noted that the scan 1 was skewed toward later gestational ages in the CHD group and earlier gestational ages in the Control group. Thus, individuals on the extremes of both groups were removed from final analysis to ensure groups were balanced in terms of age at scan and sex.

Surface Generation

The reconstructed anatomical images and manually refined segmentations were used to generate a three-dimensional surface representation of the cortical midthickness segmentation for each hemisphere using Caret ((Van Essen et al. 2001); Figure 1E). A closed contour "medial wall" boundary was drawn on a flattened surface along the boundary of the corpus callosum, basal forebrain, and the fundus of the parahippocampal fissure. Cortical surface area (CSA) was calculated from the cortical midthickness surface, excluding the medial wall as previously described (Ortinau et al. 2013). A cerebral hull surface was also generated in Caret which runs along the outer parameter of the gyri without sinking into the sulci. Gyrification index (GI) was calculated as the cortical midthickness surface area divided by the cerebral hull surface area. Mean curvature and sulcal depth maps were generated from cortical midthickness surfaces using CARET software and Connectome Workbench.

Longitudinal Analysis

To obtain longitudinal point correspondence between the two cortical midthickness surfaces (generated from MRI 1 and MRI 2) for each individual, younger and older surfaces were registered using anatomically-constrained Multimodal Surface Matching, aMSM (Garcia et al. 2018; Robinson et al. 2018). Matching was defined using mean curvatures and manually-modified medial wall delineations, and control mesh regularization was defined to minimize strain energy associated with the deformation between younger and older area-normalized cortical midthickness surfaces as described in Garcia et al. (Garcia et al. 2018). The resulting longitudinally-registered surfaces were used to generate detailed surface expansion maps for each subject. Surface expansion was defined as the ratio of older to younger surface area for each triangle on the control mesh. To prevent bias associated with the direction of registration, final maps were generated by averaging results of longitudinal registration from both older to younger and younger to older directions (Garcia et al. 2018). Final surface expansion maps were also transformed to calculate growth rate (defined as the percent surface expansion at each point divided by weeks between MRI 1 and MRI 2) and relative expansion (defined as surface expansion at each point divided by the global expansion for each individual hemisphere) (Garcia et al. 2018).

Cross-sectional Analysis

To facilitate group-level comparisons of growth rate and relative expansion, all individual surfaces were registered to a study-specific atlas, which was generated using aMSM according to previously described methods (Garcia et al. 2018). Briefly, unregistered MRI 1 surfaces were combined to generate an initial average surface, to which all MRI 1 surfaces were then aMSM-registered. The resulting aMSM-registered surfaces were then combined to generate a refined average surface (study-specific atlas). MRI 1 surfaces and corresponding growth maps for each individual were then registered again to the study-specific atlas. To ensure balanced representation of CHD and control subjects in both initial and refined atlas generation, average surfaces were generated separately for the CHD and control groups, then average CHD and average control surfaces were averaged, such that the result is a weighted average comprised of 50% CHD, 50% Control.

Finally, since previous studies of cortical differences in patients with CHD have largely focused on birth or later time points (Ortinau et al. 2013; Claessens et al. 2016; Kelly et al. 2017; Kelly et al. 2019; Morton et al. 2021), we also compared cortical surface morphology at fetal MRI 2 (close to birth) between CHD and control groups. Atlas-registered surfaces were compared in terms of local vertex surface area (area attributable to the individual cortical midthickness surface) and sulcal depth at each point.

Statistical analysis

For the window of development considered in this study, increases in CSA and GI with age are best described using an exponential growth curve (Figure 2). Thus, statistical models employed log-transformed values of CSA and GI as the dependent variables in a linear mixed effect regression model (R statistical software). For primary analysis, group (CHD or Control), sex (Male or Female), site (SLCH or BCH), and gestational age at scan were considered as fixed effects, and study ID was included as a random effect to account for repeated measures (two time points per subject). To account for multiple comparisons (4 independent variables of interest), the threshold for type 1 error (alpha) was set at the more stringent threshold of 0.05/4, such that fixed effects were only considered significant if $p<0.0125$.

To determine whether regional differences in growth were statistically significant between groups, atlas-registered growth maps were compared using permutation analysis of linear models (PALM) with threshold-free cluster enhancement (TFCE) using 1,000 iterations and family-wise error correction on any reported p-values. Atlas surfaces and vertex areas were used for TFCE surface area computations. Similar to global statistics, summary statistics involving relative expansion were generated from log-transformed values to ensure linearity and normally distributed data, then transformed back for final display.

To determine regions of highest and lowest growth within each group, one-sample t-tests were performed on the log transform of relative surface expansion. To determine significant differences in absolute growth rate (% expansion per week) between CHD and control groups, a two-sample t-test was considered. In all statistical comparisons, covariate effects of gestational age at MRI 1 were considered, based on potential group differences in this parameter and evidence suggesting age-related changes in the trajectory of cortical expansion during development (Garcia et al. 2018). To further confirm group differences, a two-sample t-test was conducted on a subset of age-matched subjects (Supplement). For comparisons focused on MRI 2, gestational age was well balanced between CHD and Control groups, such that no corrections were needed.

Results

Cohort Characteristics

One hundred ten fetuses (71 from BCH and 39 from SLCH) met inclusion criteria, but 44 (32 from BCH and 12 from SLCH) had insufficient MRI quality for cortical analysis at first or second scan. Of the remaining 66 fetuses, final analyses were conducted on 60 fetuses that were age- and sex-matched by study group. This resulted in a total of 36 fetuses with complex CHD (23 from BCH and 13 from SLCH) and 24 controls (16 from BCH and eight from SLCH; 22 with family history of CHD). Cohort characteristics were comparable between groups (Table 1). For the CHD group, eight (22%) were HLHS, 10 (28%) were TGA, seven (19%) were TOF, and 11 (42%) were Other CHD. Other CHD diagnoses included two with complex single ventricle, two with atrioventricular canal defect, three with coarctation of the aorta (one with a ventricular septal defect), one with double outlet right ventricle, one with double inlet left ventricle, one with aortic stenosis with evolving HLHS, and one with truncus arteriosus.

As illustrated in Figure 2, plotting all data points (MRI 1 and MRI 2 for each subject) revealed approximately exponential increases in both CSA and GI over time (Table 2). Linear mixed effect regression revealed strong effects of gestational age at MRI ($p<1e\text{-}15$) on CSA and GI, with CSA increasing exponentially at a rate of approximately 11% per week and GI increasing exponentially at approximately 4% per week in both hemispheres. Smaller but significant group effects were also observed ($p<0.01$ in both hemispheres), such that both CSA and GI were significantly reduced in the CHD group (approximately 6% for CSA, 2% for GI). A weak effect of fetal sex was observed, such that CSA was slightly lower among females, but this did not reach our threshold for significance in either hemisphere. Site effects did not reach the threshold of significance for any metric.

Regional patterns of cortical expansion during typical fetal development

To examine regional patterns of cortical expansion, we first focused on the control group. As illustrated in Figure 3A–B, subject-specific cortical expansion maps were generated for each control fetus, and relative expansion maps were plotted to highlight regions of relatively high and low expansion within the cortex. First, trends in typical fetal development were assessed by comparing relative expansion maps for all fetuses in the control group (Figure 3C). Over the developmental period considered, expansion was generally high in temporal and parietal regions and low in visual and prefrontal cortices. However, significant effects were observed for gestational age at MRI 1. Expansion of central cortical regions (pre/post central gyri, insula) was more pronounced for fetuses scanned at earlier gestational ages (26–29 weeks) for MRI 1, while expansion of more anterior or posterior regions (prefrontal and visual cortices) was more pronounced for fetuses scanned at later gestational ages (30–32 weeks) for MRI 1, reflecting a later developmental window from MRI 1 to MRI 2.

Regional differences in cortical expansion between fetuses with and without congenital heart defects

As illustrated in Figure 2, total CSA was generally higher in healthy controls than in fetuses with CHD. To examine regional differences between the CHD and control groups, we considered cortical expansion rate, defined as percent cortical expansion from MRI 1 to MRI 2 divided by the number of weeks between MRI 1 and MRI 2. As shown in Figure 4A, the CHD group demonstrated slower cortical expansion than controls, which was most apparent in areas of highest relative expansion among control fetuses (see Fig. 3). After accounting for effects of gestational age at MRI 1, reductions in expansion rate associated with CHD were localized to the lateral temporal and occipital lobes, with more pronounced differences in the right hemisphere (Figure 4B). While group differences did not reach statistical significance after family-wise error correction (to account for comparisons at each vertex on the cortical surface), emerging trends support a gradient effect in which cortical expansion rate is relatively reduced in temporal and posterior regions and may be slightly increased in more anterior regions for fetuses with CHD.

Author Manuscript
Author Manuscript
Author Manuscript

We note that within the CHD group, high variability was observed in the individual maps of cortical expansion, with some appearing similar to age-matched controls and some exhibiting pronounced reductions in cortical growth of specific regions. To further visualize differences between types of CHD and Controls, we directly compared individual cortical expansion maps generated from similar gestational ages at MRI 1 and MRI 2 (Figure 5). Based on available data, the window of 30 (29.43–30.71) weeks to 37 (36.43–37.86) weeks offered the most subjects, including 11 CHD subjects with diagnosis of HLHS (2), TGA (2), TOF (4), Other CHD (3), and 4 controls. Within each group, the brain with the highest relative expansion (red, orange, or yellow color) of right lateral temporal lobe was selected for visual comparison as the “fast expanding”. Similarly, the brain with lowest relative expansion (blue or green) in this region was selected as the “slow expanding”. If more than one brain qualified for fastest or slowest expansion rate, the brain with the most typical shape was selected to represent that expansion rate.

Regional differences in cortical area and folding in late gestation among fetuses with and without congenital heart defects

When comparing cortical morphology in CHD relative to Control subjects at late gestation (Figure 6A), local surface area was reduced by up to 10% in some regions of the brain, particularly the right temporal and occipital lobes. Similar but less pronounced effects were observed on the left hemisphere. This spatial pattern is consistent with trends observed in cortical expansion rate (Figure 4). Similarly, we considered sulcal depth differences between CHD and Control groups, defined as the difference in average sulcal depth between the CHD and Control groups. Comparisons revealed reduced sulcal depth (Figure 6B) in the superior temporal sulcus of the left hemisphere, but not right hemisphere, among fetuses with CHD relative to controls. Reductions of similar magnitude were observed in the calcarine and parieto-occipital sulci, as well as along the frontal border of the insula, in the right hemisphere.

Discussion

The current study is the first to reveal spatiotemporal patterns of cortical expansion in human fetuses using aMSM. In analysis focused on typically developing fetuses (Figure 3), this methodologic approach identified regions of fastest expansion in utero over the third trimester, as well as a time-sensitive gradient of cortical expansion. For fetuses with CHD, global metrics of cortical development demonstrated reduced cortical expansion and gyrification from mid to late gestation when compared to controls. Regional comparisons between controls and fetuses with CHD revealed a particular vulnerability of the temporal lobe, reflected by decreased cortical expansion, surface area, and sulcal depth. These findings provide a framework for understanding typical fetal cortical development and emphasize the importance of investigating longitudinal changes within individual fetuses, which may delineate departures from the typical developmental trajectory that could ultimately inform risk for neurodevelopmental impairments in the future.

Spatiotemporal patterns of cortical expansion in human fetuses

During the period of fetal brain development considered in this study (approximately 29 to 36 weeks GA, on average), typically developing fetuses displayed greatest expansion in temporal and parietal regions. This finding is consistent with patterns previously reported in very preterm infants (Garcia et al. 2018), who were analyzed over a similar developmental window (27 to 38 weeks postmenstrual age), using the same approach for longitudinal registration and cortical expansion mapping (aMSM). Moreover, in this study we leveraged variability in the timing of MRI 1 (actual range 26 to 32 weeks GA) to quantify dynamic shifts in the pattern of cortical expansion. We found that expansion of central cortical regions was more pronounced for fetuses who underwent MRI at 26–29 weeks GA, while expansion of more anterior or posterior regions was more pronounced at later gestational ages (30–32 weeks GA). This timing is also consistent with dynamic shifts previously reported in very preterm infants, for whom three distinct time windows could be measured (Garcia et al. 2018). Recent work in the ferret, an emerging model system for the study of cortical folding, has applied even more detailed longitudinal sampling (6 MRI scans per animal) to characterize the full trajectory of cortical expansion over a roughly equivalent developmental period (Garcia et al. 2024). Similar dynamics were again observed in this case, with an early peak in cortical expansion among primary motor and somatosensory cortices and a later peak among frontal and occipital brain regions. These differences in developmental timing are supported by studies of cortical maturation (as measured by cortical diffusion) in human and animal models (Deipolyi et al. 2005; Kroenke et al. 2009), as well as timing of developing functional networks in human (Ball et al. 2014).

Despite this consistency across clinical cohorts and species, one notable deviation between preterm and fetal trajectories was observed: Previous studies have found visual cortex expansion to be relatively high, particularly from 27–30 weeks, in preterm infants (Garcia et al. 2018) and postnatal ferrets (Garcia et al. 2024), but not in fetuses of the present study. This discrepancy could relate to biological differences between preterm and fetal developmental trajectories, as preterm infants (and ferrets) are exposed to ex-utero visual stimuli relatively early, compared to human fetuses. However, differences in MRI acquisition parameters and processing across the two studies caution against direct comparison. While the present work provides the first glance at cortical expansion trajectories in utero, future studies are needed to directly explore and understand differences between fetal and preterm human cortical development.

Reductions observed among CHD fetuses compared to controls

Most investigations of fetal brain development in CHD have focused on qualitative metrics, such as maturation scoring (Jaimes et al. 2020), or have employed in utero methods for measuring total and regional brain volumes (Limperopoulos et al. 2010; Sun et al. 2015; Rollins et al. 2021). Fewer studies have examined cortical measures, largely due to a lack of automated approaches for defining the boundaries of the fetal cortex, which requires time-intensive manual analyses and optimized imaging acquisition for cortical segmentation. Nonetheless, manual approaches have been informative, demonstrating reduced cortical volume, surface area, and gyrification; delayed emergence of sulci; and aberrations in sulcal patterns for fetuses with CHD (Clouchoux et al. 2013; Ortinau et al. 2019; Rollins et al.

2021). This study provides a significant contribution to current literature by examining change over time within individual fetuses, an approach that has only been feasible for postnatal imaging to date.

By considering change over time within subjects, we found that the rates of cortical expansion and gyrification were significantly reduced in CHD fetuses compared to controls (Figure 2, Table 2). Preclinical and neonatal CHD data show a clear association of lower cerebral oxygen delivery with reduced cortical volume (Kelly et al. 2017) and altered cortical microstructure (Kelly et al. 2019), supporting a link between cerebral hypoxia and cortical development. Fetal brain compartments containing neuroprogenitor cells (proliferative compartments), pre-myelinating oligodendrocytes (intermediate zone), and subplate neurons (subplate zone) are particularly impacted for the fetus with CHD, especially for diagnoses associated with impaired cerebral substrate delivery (Rollins et al. 2021). These compartments play a crucial role in cortical development and cerebral connectivity. Thus, it is plausible that early disturbances in these transient fetal brain regions, due to altered cerebral substrate delivery, contribute to slower rates of cortical expansion in CHD. Alternatively, or in addition, impaired cardiac hemodynamics may directly affect cortical neurons. Finally, genetic factors may also influence cortical development in CHD. Abnormal sulcal patterns have been associated with adverse neurodevelopmental outcomes in children and adolescents CHD, particularly for patients with damaging de novo variants on whole exome sequencing (Morton et al. 2020; Morton et al. 2021). These same cortical abnormalities are seen in fetuses with CHD and occur in early emerging sulci that are generally under tighter genetic control (Ortinau et al. 2019).

For any of these factors, effects on the brain could be global or localized in specific brain regions. By comparing individualized maps of cortical expansion, we found that reduced expansion is most pronounced in the right temporal lobe, accompanied by more subtle reductions in the left temporal and surrounding posterior regions. This was confirmed by cross-sectional analysis of final surface area and sulcal depth at MRI 2, where CHD fetuses exhibited up to 10% less surface area in right temporal and occipital regions and reduced folding in the left temporal, right occipital, and right insular cortices. These findings could suggest a regional vulnerability or may reflect that regions developing most rapidly are those regions where differences can be readily detected.

The right temporal region is believed to play an important role in facial recognition and emotional processing (Gainotti 2007; Borghesani et al. 2019; Reisch, Wegrzyn, Mielke, Mehlmann, Woermann, Bien, et al. 2022; Reisch, Wegrzyn, Mielke, Mehlmann, Woermann, Kissler, et al. 2022), such that cortical expansion differences observed in this region may contribute to the developmental and social cognition deficits that have been well documented among CHD populations (Sigmon et al. 2019; Gonzalez et al. 2021). However, outcomes vary greatly across individuals (Sood et al. 2024). In the present study, we highlight temporal lobe reductions that emerged in group analysis, but we also note that many CHD fetuses exhibited cortical expansion falling within normal limits (Figure 5). This variability across and within CHD diagnosis groups may mirror the variability in clinical neurodevelopmental outcomes among individuals with CHD. Future work should assess whether underdevelopment of the right temporal lobe, measured during fetal development at the individual patient level, may serve as a useful biomarker to predict increasing risk for neurodevelopmental disorders.

Implications for cortical expansion on cortical and subcortical morphology

In this study, we focused on cortical expansion to quantify differences between CHD and healthy control fetuses, due to its proposed role as a driver of morphological changes including gyrification and subcortical growth. While several mechanisms have been proposed to drive brain folding, one leading hypothesis is that expansion of cortex, constrained by slower growing subcortical tissues, induces gyrification through buckling (Richman et al. 1975). In an extension of this hypothesis, our recent work has proposed that the expanding cortex pulls on subcortical tissues to induce growth and remodeling of the prospective white matter (Garcia et al. 2021). Moreover, if the rate of cortical expansion is reduced, subcortical tissues may grow at a speed that accommodates cortical expansion, such that gyrification is prevented or reduced (Bayly et al. 2013).

Consistent with these dynamics, the present study found that global reduction in cortical expansion among CHD individuals was accompanied by global reduction in GI. Previous studies have also reported delayed or reduced sulcation in CHD, and several have specifically noted alterations in the temporal, insular, and occipital lobes (Clouchoux et al. 2013; Ortinau et al. 2013; Ortinau et al. 2019). We found that cortical expansion was most dramatically reduced in a similar region, accompanied by sulcal depth alterations in this region.

The left-right asymmetry observed in our analysis, particularly in the temporal lobe, is consistent with trends observed in previous developmental studies (Dubois et al. 2008; Im et al. 2010; Kasprian et al. 2011; Habas et al. 2012; Yun et al. 2022). For example, emergence of the superior temporal sulcus, and to a lesser degree other temporal sulci, is delayed on the left hemisphere compared to the right (Yun et al. 2022). Our finding of increased expansion in the right temporal lobe is consistent with earlier emergence of folds in this hemisphere. Moreover, while our analysis suggests that differences in cortical expansion between CHD and control are more pronounced in the right hemisphere (over the period of consideration), differences in sulcal depth were more pronounced on the left at the end of gestation. This apparent paradox could be explained by the dynamics of cortical expansion and folding: If sulci of the right temporal lobe are relatively well formed before the period of observed fetal growth reduction, but sulci of the left temporal lobe continue to form and deepen during this period, sulci of the left may be more susceptible to expansion-driven deviations in folding. While robust models or additional mechanisms may be necessary to explain these subtleties, the current findings of regionally reduced cortical expansion provide valuable context for studies seeking to interpret local morphological differences between individuals with CHD compared to controls.

Limitations

Limitations of this study include a relatively small sample size (n=60 total fetuses) and wide range of gestational ages for MRI 1 acquisition. A larger sample, or conversely tighter control in gestational age at scan between groups, would be expected to increase statistical power for detection of differences between groups. However, we stress that the longitudinal nature of the present analysis, which allows direct calculation of cortical change within an individual subject, offers a degree of sensitivity not possible with larger, existing cross-sectional cohorts. Future studies of fetal brain development should prioritize longitudinal acquisition and analysis to capture within-subject changes in larger cohorts. Of note, our present study leveraged cross-sectional differences in gestational age at scan to uncover changes in cortical expansion over time. However, direct capture of within-individual cortical expansion changes over distinct gestational windows, as previously considered in preterm infants (Garcia et al. 2018), may offer more robust insights. Future studies should consider capture of more than two fetal time points to allow calculation of within-subject changes in cortical expansion over discrete windows of fetal development and to potentially explore changes in earlier periods of gestation (<26 weeks).

Conclusion

Data on fetal cortical expansion has only begun to be reported within the past few years. We used longitudinal fetal imaging, along with novel segmentation and physics-based registration approaches, to quantify cortical expansion and gyrification within individual fetuses and assess regional differences for those with CHD. Comparison between CHD and control subjects revealed global reductions in cortical size and gyrification, as well as localized reductions in the cortical expansion and gyrification of key regions. These results may offer insight into the developmental periods and specific brain regions of highest vulnerability in CHD, which may guide understanding of mechanisms underlying neurodevelopmental impairment and ultimately aid in risk stratification. Future investigations using larger sample sizes, wider gestational age windows, and more MRI timepoints may lend further refinement of regional differences and enable analyses by cerebral substrate delivery.

Acknowledgements

We would like to thank Reni Akande, Anthony Alfonso, and Arieona Witherspoon for their contributions to manual post-processing of data collected in this study.

Funding

This work was supported the National Institutes of Health including the National Institute of Neurological Disorders and Stroke (K23 NS101120 and R01 NS121334 to C.K.R., R01 NS133116 to K.E.G.), the National Heart, Lung, and Blood Institute (K23 HL141602 to C.M.O, R01EB018988 and R01NS106030 to A.G.), and the McKnight Foundation Technological Innovations in Neuroscience Award to A.G., the Office of Faculty Development at Boston Children's Hospital Career Development Awards to A.G. and C.K.R., the Mend A Heart Foundation to C.M.O., the Galloway Foundation to K.E.G., and the Kenrose Kitchen Table Foundation to C.K.R. The content does not necessarily represent the official views of the National Institutes of Health or other funding agencies.

References

Andescavage NN, du Plessis A, McCarter R, Serag A, Evangelou I, Vezina G, Robertson R, Limperopoulos C. 2017. Complex Trajectories of Brain Development in the Healthy Human Fetus. Cereb Cortex. 27:5274–5283. [PubMed: 27799276]

Andescavage NN, Pradhan S, Gimovsky AC, Kapse K, Donofrio MT, Cheng JJ, Sharker Y, Wessel D, du Plessis AJ, Limperopoulos C. 2023. Magnetic Resonance Spectroscopy of Brain Metabolism in Fetuses With Congenital Heart Disease. J Am Coll Cardiol. 82:1614–1623. [PubMed: 37821172]

Asschenfeldt B, Evald L, Heiberg J, Salvig C, Ostergaard L, Dalby RB, Eskildsen SF, Hjortdal VE. 2020. Neuropsychological Status and Structural Brain Imaging in Adults With Simple Congenital Heart Defects Closed in Childhood. J Am Heart Assoc. 9:e015843. [PubMed: 32427039]

Ball G, Aljabar P, Zebari S, Tusor N, Arichi T, Merchant N, Robinson EC, Ogundipe E, Rueckert D, Edwards AD. 2014. Rich-club organization of the newborn human brain. Proceedings of the National Academy of Sciences. 111:7456–7461.

Bayly PV, Okamoto RJ, Xu G, Shi Y, Taber LA. 2013. A cortical folding model incorporating stress-dependent growth explains gyral wavelengths and stress patterns in the developing brain. Phys Biol. 10:016005. [PubMed: 23357794]

Borghesani V, Narvid J, Battistella G, Shwe W, Watson C, Binney RJ, Sturm V, Miller Z, Mandelli ML, Miller B, Gorno-Tempini ML. 2019. “Looks familiar, but I do not know who she is”: The role of the anterior right temporal lobe in famous face recognition. Cortex. 115:72–85. [PubMed: 30772608]

Claessens NH, Moeskops P, Buchmann A, Latal B, Knirsch W, Scheer I, Isgum I, de Vries LS, Benders MJ, von Rhein M. 2016. Delayed cortical gray matter development in neonates with severe congenital heart disease. Pediatr Res. 80:668–674. [PubMed: 27434120]

Clouchoux C, du Plessis AJ, Bouyssi-Kobar M, Tworetzky W, McElhinney DB, Brown DW, Gholipour A, Kudelski D, Warfield SK, McCarter RJ, Robertson RL Jr, Evans AC, Newburger JW, Limperopoulos C. 2013. Delayed cortical development in fetuses with complex congenital heart disease. Cereb Cortex. 23:2932–2943. [PubMed: 22977063]

Deipolyi AR, Mukherjee P, Gill K, Henry RG, Partridge SC, Veeraraghavan S, Jin H, Lu Y, Miller SP, Ferriero DM, Vigneron DB, Barkovich AJ. 2005. Comparing microstructural and macrostructural development of the cerebral cortex in premature newborns: diffusion tensor imaging versus cortical gyration. Neuroimage. 27:579–586. [PubMed: 15921934]

Dou H, Karimi D, Rollins CK, Ortinau CM, Vasung L, Velasco-Annis C, Ouaalam A, Yang X, Ni D, Gholipour A. 2020. A deep attentive convolutional neural network for automatic cortical plate segmentation in fetal MRI. IEEE transactions on medical imaging. 40:1123–1133.

Dubois J, Benders M, Cachia A, Lazeyras F, Ha-Vinh Leuchter R, Sizonenko SV, Borradori-Tolsa C, Mangin J-F, Hüppi PS. 2008. Mapping the early cortical folding process in the preterm newborn brain. Cerebral cortex. 18:1444–1454. [PubMed: 17934189]

Gainotti G 2007. Face familiarity feelings, the right temporal lobe and the possible underlying neural mechanisms. Brain Res Rev. 56:214–235. [PubMed: 17822771]

Garcia KE, Robinson EC, Alexopoulos D, Dierker DL, Glasser MF, Coalson TS, Ortinau CM, Rueckert D, Taber LA, Van Essen DC, Rogers CE, Smyser CD, Bayly PV. 2018. Dynamic patterns of cortical expansion during folding of the preterm human brain. Proc Natl Acad Sci U S A. 115:3156–3161. [PubMed: 29507201]

Garcia KE, Wang X, Kroenke CD. 2021. A model of tension-induced fiber growth predicts white matter organization during brain folding. Nat Commun. 12:6681. [PubMed: 34795256]

Garcia KE, Wang X, Santiago SE, Bakshi S, Barnes AP, Kroenke CD. 2024. Longitudinal MRI of the developing ferret brain reveals regional variations in timing and rate of growth. Cereb Cortex. 34.

Gholipour A, Rollins CK, Velasco-Annis C, Ouaalam A, Akhondi-Asl A, Afacan O, Ortinau CM, Clancy S, Limperopoulos C, Yang E, Estroff JA, Warfield SK. 2017. A normative spatiotemporal MRI atlas of the fetal brain for automatic segmentation and analysis of early brain growth. Sci Rep. 7:476. [PubMed: 28352082]

Gonzalez VJ, Kimbro RT, Cutitta KE, Shabosky JC, Bilal MF, Penny DJ, Lopez KN. 2021. Mental Health Disorders in Children With Congenital Heart Disease. Pediatrics. 147.

Habas PA, Scott JA, Roosta A, Rajagopalan V, Kim K, Rousseau F, Barkovich AJ, Glenn OA, Studholme C. 2012. Early folding patterns and asymmetries of the normal human brain detected from in utero MRI. Cerebral cortex. 22:13–25. [PubMed: 21571694]

Im K, Jo HJ, Mangin J-F, Evans AC, Kim SI, Lee J-M. 2010. Spatial distribution of deep sulcal landmarks and hemispherical asymmetry on the cortical surface. Cerebral cortex. 20:602–611. [PubMed: 19561060]

Jaimes C, Rofeberg V, Stopp C, Ortinau CM, Gholipour A, Friedman KG, Tworetzky W, Estroff J, Newburger JW, Wypij D, Warfield SK, Yang E, Rollins CK. 2020. Association of Isolated

Congenital Heart Disease with Fetal Brain Maturation. AJNR Am J Neuroradiol. 41:1525–1531. [PubMed: 32646947]

Kainz B, Steinberger M, Wein W, Kuklisova-Murgasova M, Malamateniou C, Keraudren K, Torsney-Weir T, Rutherford M, Aljabar P, Hajnal JV, Rueckert D. 2015. Fast Volume Reconstruction From Motion Corrupted Stacks of 2D Slices. IEEE Trans Med Imaging. 34:1901–1913. [PubMed: 25807565]

Kasprian G, Langs G, Brugger PC, Bittner M, Weber M, Arantes M, Prayer D. 2011. The prenatal origin of hemispheric asymmetry: an in utero neuroimaging study. Cerebral cortex. 21:1076–1083. [PubMed: 20851852]

Kelly C, Toro R, Di Martino A, Cox CL, Bellec P, Castellanos FX, Milham MP. 2012. A convergent functional architecture of the insula emerges across imaging modalities. Neuroimage. 61:1129–1142. [PubMed: 22440648]

Kelly CJ, Christiaens D, Batalle D, Makropoulos A, Cordero-Grande L, Steinweg JK, O'Muircheartaigh J, Khan H, Lee G, Victor S, Alexander DC, Zhang H, Simpson J, Hajnal JV, Edwards AD, Rutherford MA, Counsell SJ. 2019. Abnormal Microstructural Development of the Cerebral Cortex in Neonates With Congenital Heart Disease Is Associated With Impaired Cerebral Oxygen Delivery. J Am Heart Assoc. 8:e009893. [PubMed: 30821171]

Kelly CJ, Makropoulos A, Cordero-Grande L, Hutter J, Price A, Hughes E, Murgasova M, Teixeira R, Steinweg JK, Kulkarni S, Rahman L, Zhang H, Alexander DC, Pushparajah K, Rueckert D, Hajnal JV, Simpson J, Edwards AD, Rutherford MA, Counsell SJ. 2017. Impaired development of the cerebral cortex in infants with congenital heart disease is correlated to reduced cerebral oxygen delivery. Sci Rep. 7:15088. [PubMed: 29118365]

Kroenke CD, Taber EN, Leigland LA, Knutsen AK, Bayly PV. 2009. Regional patterns of cerebral cortical differentiation determined by diffusion tensor MRI. Cereb Cortex. 19:2916–2929. [PubMed: 19363145]

Lefevre J, Germanaud D, Dubois J, Rousseau F, de Macedo Santos I, Angleys H, Mangin JF, Huppi PS, Girard N, De Guio F. 2016. Are Developmental Trajectories of Cortical Folding Comparable Between Cross-sectional Datasets of Fetuses and Preterm Newborns? Cereb Cortex. 26:3023–3035. [PubMed: 26045567]

Limperopoulos C, Tworetzky W, McElhinney DB, Newburger JW, Brown DW, Robertson RL Jr, Guizard N, McGrath E, Geva J, Annese D, Dunbar-Masterson C, Trainor B, Laussen PC, du Plessis AJ. 2010. Brain volume and metabolism in fetuses with congenital heart disease: evaluation with quantitative magnetic resonance imaging and spectroscopy. Circulation. 121:26–33. [PubMed: 20026783]

Morton SU, Maleyeff L, Wypij D, Yun HJ, Newburger JW, Bellinger DC, Roberts AE, Rivkin MJ, Seidman JG, Seidman CE, Grant PE, Im K. 2020. Abnormal Left-Hemispheric Sulcal Patterns Correlate with Neurodevelopmental Outcomes in Subjects with Single Ventricular Congenital Heart Disease. Cereb Cortex. 30:476–487. [PubMed: 31216004]

Morton SU, Maleyeff L, Wypij D, Yun HJ, Rollins CK, Watson CG, Newburger JW, Bellinger DC, Roberts AE, Rivkin MJ, Grant PE, Im K. 2021. Abnormal Right-Hemispheric Sulcal Patterns Correlate with Executive Function in Adolescents with Tetralogy of Fallot. Cereb Cortex. 31:4670–4680. [PubMed: 34009260]

Ortinau C, Alexopoulos D, Dierker D, Van Essen D, Beca J, Inder T. 2013. Cortical folding is altered before surgery in infants with congenital heart disease. J Pediatr. 163:1507–1510. [PubMed: 23988135]

Ortinau CM, Rollins CK, Gholipour A, Yun HJ, Marshall M, Gagoski B, Afacan O, Friedman K, Tworetzky W, Warfield SK, Newburger JW, Inder TE, Grant PE, Im K. 2019. Early-Emerging Sulcal Patterns Are Atypical in Fetuses with Congenital Heart Disease. Cereb Cortex. 29:3605–3616. [PubMed: 30272144]

Ortinau CM, Smyser CD, Arthur L, Gordon EE, Heydarian HC, Wolovits J, Nedrelow J, Marino BS, Levy VY. 2022. Optimizing Neurodevelopmental Outcomes in Neonates With Congenital Heart Disease. Pediatrics. 150.

Reillo I, de Juan Romero C, Garcia-Cabezas MA, Borrell V. 2011. A role for intermediate radial glia in the tangential expansion of the mammalian cerebral cortex. Cereb Cortex. 21:1674–1694. [PubMed: 21127018]

Reisch LM, Wegrzyn M, Mielke M, Mehlmann A, Woermann FG, Bien CG, Kissler J. 2022. Face processing and efficient recognition of facial expressions are impaired following right but not left anteromedial temporal lobe resections: Behavioral and fMRI evidence. Neuropsychologia. 174:108335. [PubMed: 35863496]

Reisch LM, Wegrzyn M, Mielke M, Mehlmann A, Woermann FG, Kissler J, Bien CG. 2022. Effects of left and right medial temporal lobe resections on hemodynamic correlates of negative and neutral scene processing. Hum Brain Mapp. 43:3293–3305. [PubMed: 35384132]

Richman DP, Stewart RM, Hutchinson JW, Caviness VS Jr. 1975. Mechanical model of brain convolutional development. Science. 189:18–21. [PubMed: 1135626]

Robinson EC, Garcia K, Glasser MF, Chen Z, Coalson TS, Makropoulos A, Bozek J, Wright R, Schuh A, Webster M, Hutter J, Price A, Cordero Grande L, Hughes E, Tusor N, Bayly PV, Van Essen DC, Smith SM, Edwards AD, Hajnal J, Jenkinson M, Glocker B, Rueckert D. 2018. Multimodal surface matching with higher-order smoothness constraints. Neuroimage. 167:453–465. [PubMed: 29100940]

Rollins CK, Ortinau CM, Stopp C, Friedman KG, Tworetzky W, Gagoski B, Velasco-Annis C, Afacan O, Vasung L, Beaute JI, Rofeberg V, Estroff JA, Grant PE, Soul JS, Yang E, Wypij D, Gholipour A, Warfield SK, Newburger JW. 2021. Regional Brain Growth Trajectories in Fetuses with Congenital Heart Disease. Ann Neurol. 89:143–157. [PubMed: 33084086]

Sadhwani A, Wypij D, Rofeberg V, Gholipour A, Mittleman M, Rohde J, Velasco-Annis C, Calderon J, Friedman KG, Tworetzky W, Grant PE, Soul JS, Warfield SK, Newburger JW, Ortinau CM, Rollins CK. 2022. Fetal Brain Volume Predicts Neurodevelopment in Congenital Heart Disease. Circulation. 145:1108–1119. [PubMed: 35143287]

Sigmon ER, Kelleman M, Susi A, Nylund CM, Oster ME. 2019. Congenital Heart Disease and Autism: A Case-Control Study. Pediatrics. 144.

Sood E, Newburger JW, Anixt JS, Cassidy AR, Jackson JL, Jonas RA, Lisanti AJ, Lopez KN, Peyvandi S, Marino BS. 2024. Neurodevelopmental outcomes for individuals with congenital heart disease: updates in neuroprotection, risk-stratification, evaluation, and management: a scientific statement from the American Heart Association. Circulation. 149:e997–e1022. [PubMed: 38385268]

Sun L, Macgowan CK, Sled JG, Yoo SJ, Manlhiot C, Porayette P, Grosse-Wortmann L, Jaeggi E, McCrindle BW, Kingdom J, Hickey E, Miller S, Seed M. 2015. Reduced fetal cerebral oxygen consumption is associated with smaller brain size in fetuses with congenital heart disease. Circulation. 131:1313–1323. [PubMed: 25762062]

Van Essen DC, Drury HA, Dickson J, Harwell J, Hanlon D, Anderson CH. 2001. An integrated software suite for surface-based analyses of cerebral cortex. J Am Med Inform Assoc. 8:443–459. [PubMed: 11522765]

Yun HJ, Lee HJ, Lee JY, Tarui T, Rollins CK, Ortinau CM, Feldman HA, Grant PE, Im K. 2022. Quantification of sulcal emergence timing and its variability in early fetal life: hemispheric asymmetry and sex difference. NeuroImage. 263:119629. [PubMed: 36115591]

Yushkevich PA, Piven J, Hazlett HC, Smith RG, Ho S, Gee JC, Gerig G. 2006. User-guided 3D active contour segmentation of anatomical structures: significantly improved efficiency and reliability. Neuroimage. 31:1116–1128. [PubMed: 16545965]

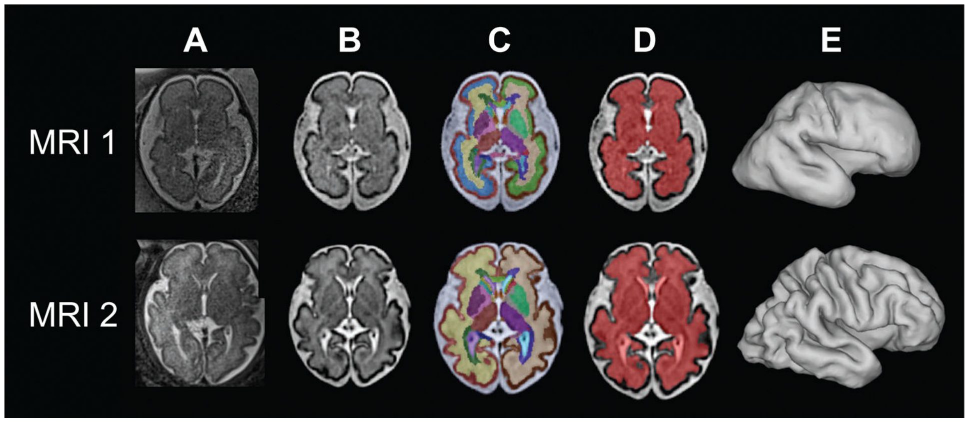

Figure 1. Image Processing and Surface Generation.

Representative images are shown at MRI 1 (top row) and MRI 2 (bottom row) for processing of raw data for surface generation. Shown are the T2wHASTE images acquired at the scanner (A), the reconstructed anatomical images (B), the automated segmentation (C), the simplified segmentations before manual refinement (D), and the cortical midthickness surfaces (E). The example shown is a CHD fetus who underwent MRI at 29 and 34 weeks gestation.

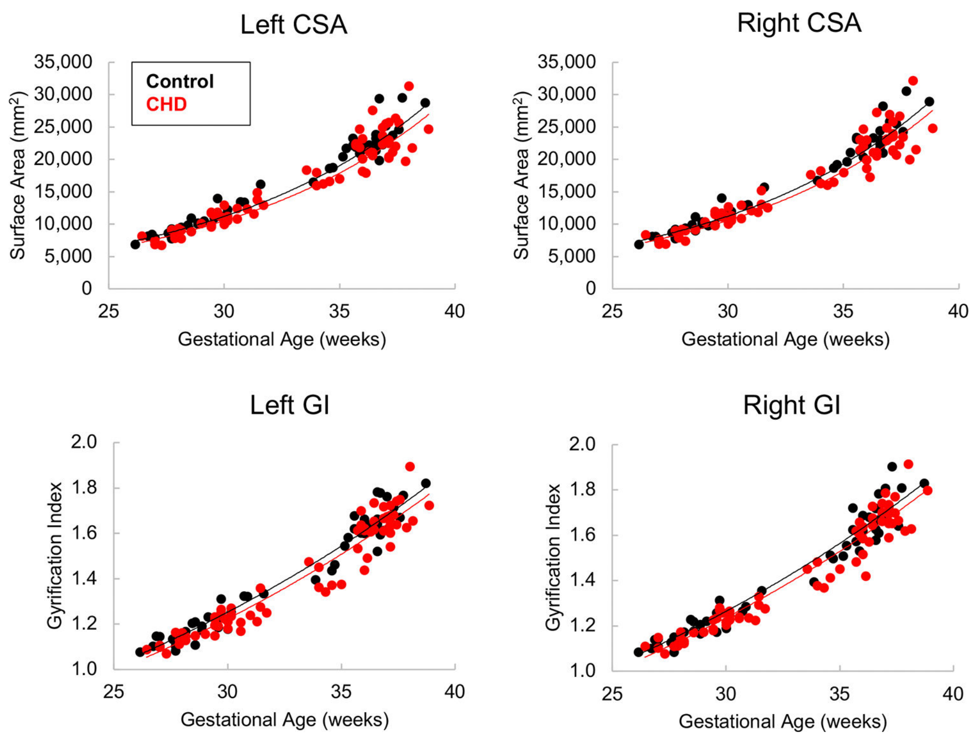

Figure 2. Differences in global metrics of cortical development, Control (n=24) and CHD (n=36).
Cortical surface area (CSA, top) and gyrification index (GI, bottom) increased approximately exponentially over the period of fetal development considered. Exponential growth curves based on mixed effects regression (Table 2) are shown for control (black) and CHD (red) groups.

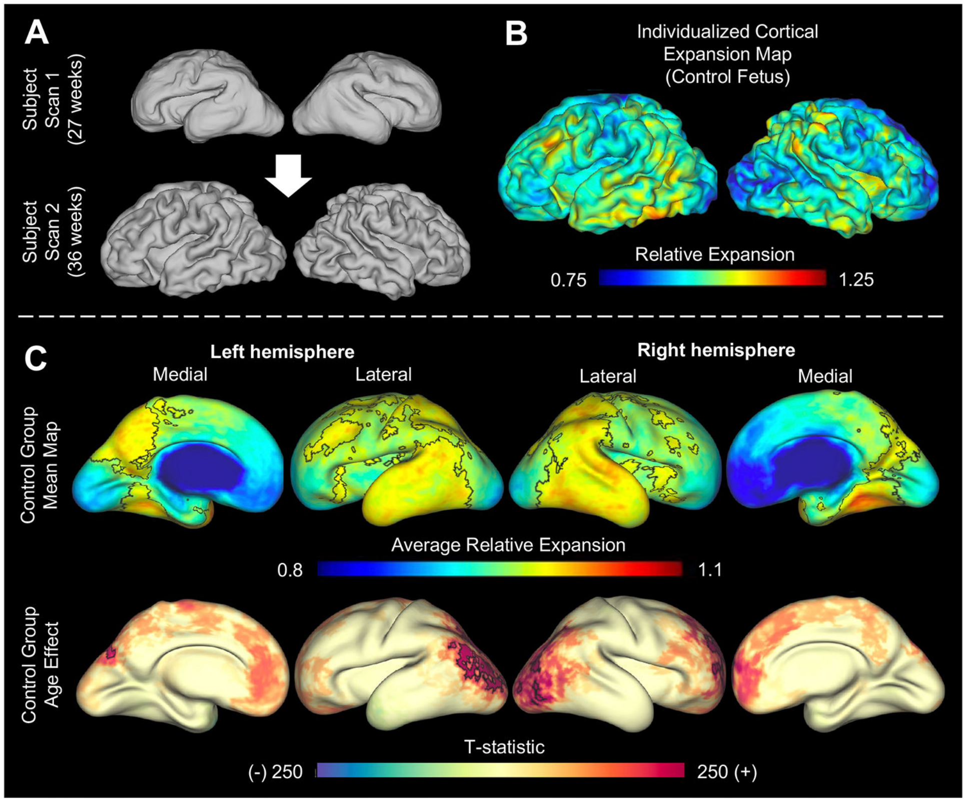

Figure 3. Cortical expansion mapping, individual and control group trends.

A-B. For each subject with cortical reconstructions at both MRI 1 and MRI 2, individualized cortical expansion maps were generated using anatomically-constrained Multimodal Surface Matching (aMSM). An illustrative example is shown for a control fetus, scanned at 27 and 36 weeks gestational age (A), resulting in the relative expansion map shown in (B). A relative expansion ratio > 1 (yellow-red) indicates regions where local cortical expansion is faster than global surface area expansion (hemisphere surface area at 36 weeks divided by hemisphere surface area at 27 weeks), and a relative expansion ratio < 1 (blue) indicates regions where local expansion is slower than global surface area expansion. **C.** Registration of all individualized maps to an atlas reveals group average trends in relative expansion among control fetuses as well as a covariate effect (t-statistic) of gestational age at MRI 1 on the pattern of expansion (bottom). Top: Black outline separates areas where local cortical expansion is significantly slower than global expansion ($p<0.05$) from areas where local cortical expansion is similar or faster than global expansion. Bottom: Warm colors (orange-magenta) indicate regions where relative expansion increases among subjects with later gestational age at MRI 1. Black outline separates areas where MRI 1 gestational age is positively correlated to increased relative expansion ($p<0.05$) from areas where MRI 1 gestational age is not correlated to relative expansion. T-statistics and p-values were calculated by using PALM with threshold-free cluster enhancement, considering a one-sample t-test with covariate effects (MRI 1 gestational age).

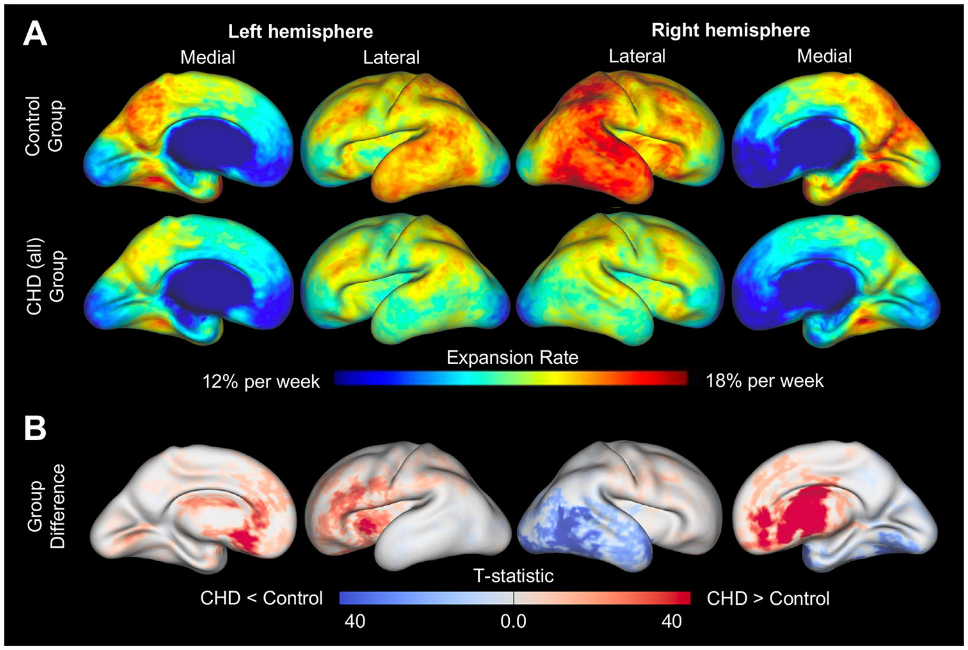

Figure 4. Cortical expansion is locally decreased in fetuses with congenital heart defects.
A. Average cortical expansion rate (% expansion per week) is shown for control (top, n=24) and CHD (bottom, n=36) groups. Regions of yellow-red indicate faster growth and regions of blue indicate slower growth. Among controls, expansion is fastest in the lateral temporal lobe of the right hemisphere, followed by the medial occipital region of the right hemisphere. Similar but less pronounced effects were observed on the left hemisphere. In the CHD cohort, expansion is reduced in both temporal lobes. **B.** Group differences in local expansion rate, revealed by two-sample t-test with covariate effects (gestational age at MRI 1). Covariate effects of MRI 1 gestational age were highly significant at almost all vertices (not shown), such that expansion rate increased with decreasing MRI 1 gestational age ($p<0.05$). While group differences were not statistically significant after correcting for MRI 1 gestational age, T-statistics revealed strong spatial trends. Blue indicates regions where growth rate was reduced in CHD relative to control, red indicates regions where growth rate was increased in CHD relative to control.

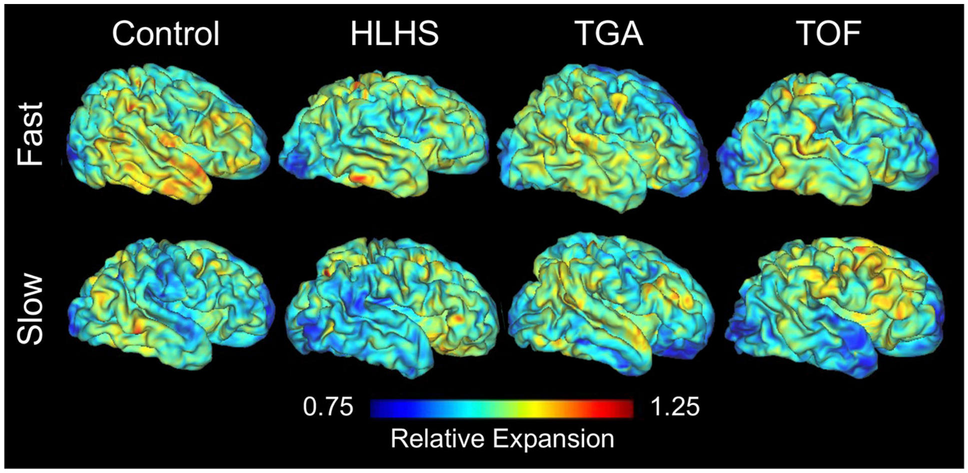

Figure 5. Expansion map variability among Control and CHD diagnoses.

Relative cortical expansion maps were compared for 8 fetuses with similar gestational ages at MRI 1 (29.43–30.71 weeks) and MRI 2 (36.43–37.86 weeks). The maps show relatively faster and slower areas of expansion within each fetus's right hemisphere. The right lateral temporal lobe, a cortical region found to expand at a greater relative rate in control fetuses compared to CHD fetuses, is juxtaposed between columns of Control, HLHS, TGA, and TOF fetuses. Within each diagnosis group, a brain with fast (top) and slow (bottom) expansion in the right lateral temporal lobe was selected to display the range of cortical patterns for each diagnosis. Great variability is present between all groups, but the general trend is upheld. Control fetuses display relatively faster right lateral temporal lobe expansion than CHD fetuses, even in the most reduced case. There was no obvious cortical expansion pattern difference between the HLHS, TGA, and TOF groups.

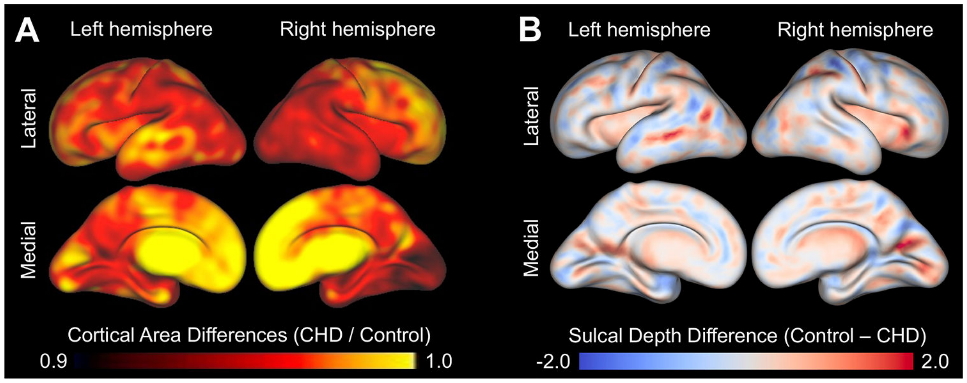

Figure 6. Cortical morphology alterations observed at MRI 2 in fetuses with congenital heart defects.

A. Ratio of vertex-wise surface area associated with CHD versus Control fetuses at MRI 2 (close to birth). Cortical area was markedly reduced by approximately 10% in the right temporal lobe, as well as in the right medial occipital lobe, of CHD fetuses relative to control fetuses (indicated by dark red-black). **B.** Comparisons of sulcal depth between CHD fetuses and control fetuses. Red indicates a reduction in sulcal depth among the CHD group, and blue indicates a complementary increase in gyral height surrounding these sulci.

Table 1.

Characteristics of the Cohort

	Control (n = 24)	CHD (n = 36)	P Value
Maternal age	32.6 (4.2)	30.7 (5.6)	0.17
Maternal race			0.16
White	22 (91.7)	29 (80.6)	
Black or African American	2 (8.3)	2 (5.6)	
Other	0 (0.0)	5 (13.9)	
Maternal ethnicity, non-Hispanic	23 (95.8)	33 (91.7)	0.64
Maternal education, college graduate	18 (75.0)	24 (66.7)	0.57
Fetal sex, male	11 (45.8)	21 (58.3)	0.43
GA at MRI 1, weeks	28.6 (1.4)	29.3 (1.4)	0.06
GA at MRI 2, weeks	36.2 (1.1)	36.4 (1.2)	0.53
GA at birth, weeks	39.2 (1.0)	39.2 (0.8)	0.85
Birth weight, grams	3534 (521)	3401 (434)	0.29
Birth head circumference, cm	34.7 (1.7)	34.3 (1.7)	0.42
Incidental findings on fetal MRI	2 (8.3)	1 (2.8)	0.68

Data are reported as mean (standard deviation) or number (percentage).

Other Maternal Race: American Indian for Alaskan Native (n=2), Asian (n=1), Mexican American (n=1), and Puerto Rican (n=1).

Incidental findings on fetal MRI included possible gyral folding abnormality (n=1 CHD), a 7mm cyst-like structure displacing the right optic nerve (n=1 control), and concern for mild spinal stenosis of unclear significance (n=1 control).

Maternal age at delivery, GA at birth, and birth measures are missing for one CHD participant.

GA=Gestational age

Author Manuscript

Author Manuscript

Author Manuscript

Table 2.

Linear mixed effects model for global surface-based metrics

Fixed Effect for Each Global Metric	Coefficient	P Value
Left Cortical Surface Area		
Gestational age at MRI (weeks)	0.1062	**<0.0001**
Group (CHD=1, Control=0)	−0.0625	**0.009**
Fetal sex (Male=1, Female=0)	0.0463	0.046
Site (SLCH=1, BCH=0)	0.0379	0.113
Right Cortical Surface Area		
Gestational age at MRI (weeks)	0.1079	**<0.0001**
Group (CHD=1, Control=0)	−0.0608	**0.010**
Fetal sex (Male=1, Female=0)	0.0486	0.034
Site (SLCH=1, BCH=0)	0.0127	0.586
Left Gyrification Index		
Gestational age at MRI (weeks)	0.0419	**<0.0001**
Group (CHD=1, Control=0)	−0.0237	**0.006**
Fetal sex (Male=1, Female=0)	0.0057	0.486
Site (SLCH=1, BCH=0)	−0.0040	0.643
Right Gyrification Index		
Gestational age at MRI (weeks)	0.0425	**<0.0001**
Group (CHD=1, Control=0)	−0.0228	**0.005**
Fetal sex (Male=1, Female=0)	0.0039	0.625
Site (SLCH=1, BCH=0)	−0.0175	0.031